NSF/RA-800442

PB81-178085

UNIVERSITY OF CALIFORNIA

SAN DIEGO

DEPARTMENT OF APPLIED MECHANICS AND ENGINEERING SCIENCES

LOCAL CHARACTERIZATION OF FREE-FIELD GROUND MOTION AND EFFECTS OF WAVE PASSAGE

By

J. E. LUCO

and

D. A. SOTIROPOULOS

A Report on Research Conducted Under Grant PFR79.00006
From the National Science Foundation

La Jolla, California

February, 1980

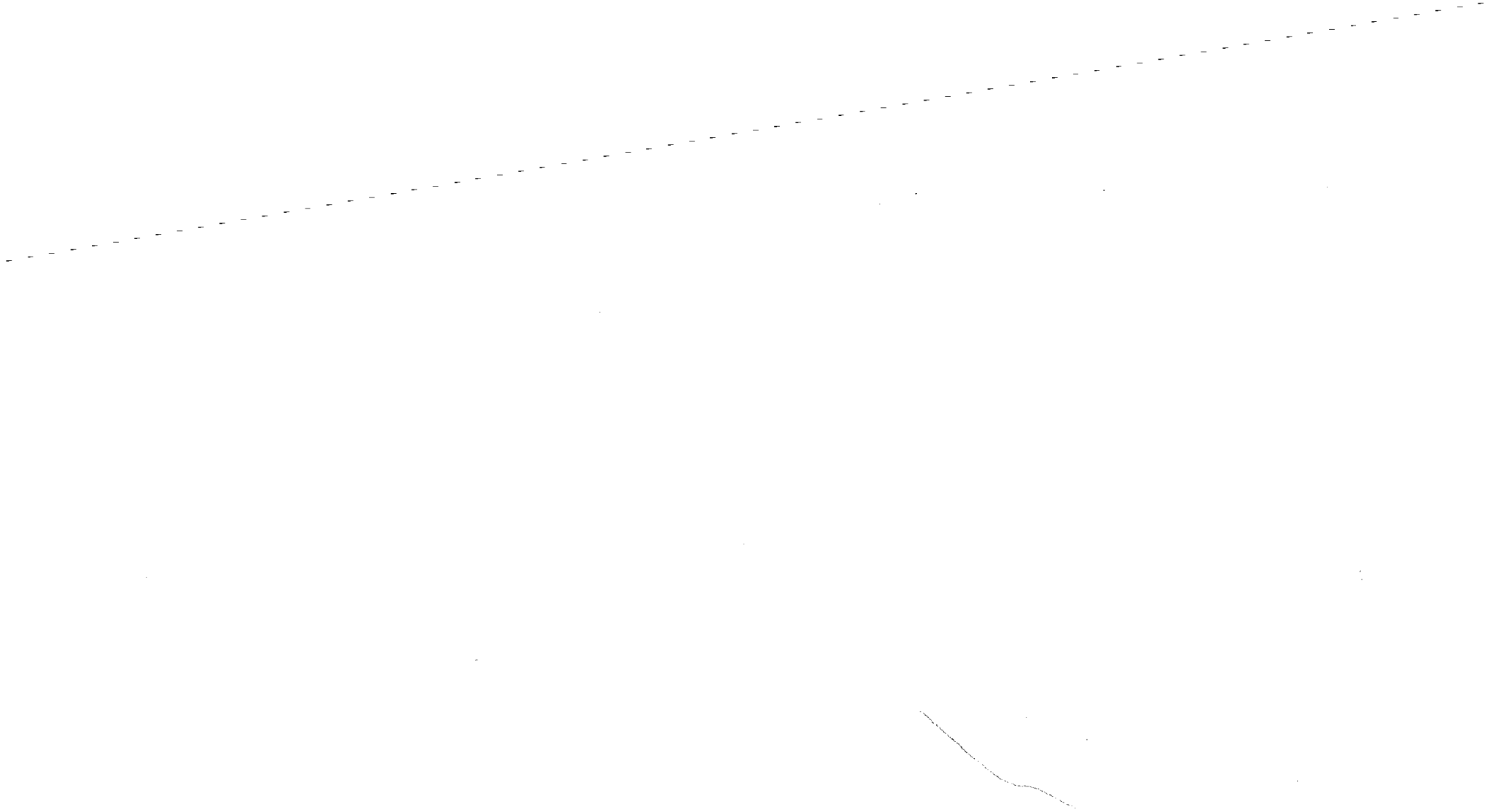

50272-101

REPORT DOCUMENTATION PAGE	1. REPORT NO. NSF/RA-800442	2.	3. Recipient's Accession No. PB81 178089

4. Title and Subtitle
Local Characterization of Free-Field Ground Motion and Effects of Wave Passage

5. Report Date
February 1980

6.

7. Author(s)
J. E. Luco, D. A. Sotiropoulos

8. Performing Organization Rept. No.

9. Performing Organization Name and Address
University of California, San Diego
Department of Applied Mechanics and Engineering Sciences
La Jolla, CA 92110

10. Project/Task/Work Unit No.

11. Contract(C) or Grant(G) No.
(C)
(G) PFR7900006

12. Sponsoring Organization Name and Address
Office of Planning and Resources Management (OPRM)
National Science Foundation
1800 G Street, N.W.
Washington, D.C. 20550

13. Type of Report & Period Covered

14.

15. Supplementary Notes

16. Abstract (Limit: 200 words)

A simple model of the seismic source and propagation medium is used to obtain a local representation of the free-field ground motion in terms of a small number of equivalent dispersive plane waves. The seismic source is represented as a dislocation distributed over a small area on a vertical fault plane. The propagation medium is represented as a layered elastic half-space. Numerical values for the equivalent phase velocities entering in the representation are included for different epicentral distances and source depths. Based on the local characterization of the free-field motion, estimates of the magnitude of the effects of nonvertically incident seismic waves on the response of foundations and structures are reported.

17. Document Analysis a. Descriptors

Earth movements
Seismic waves
Phase velocity
Structures
Wave propagation
Dynamic structural analysis
Foundations

b. Identifiers/Open-Ended Terms

Earthquake Hazards Mitigation

c. COSATI Field/Group

18. Availability Statement	19. Security Class (This Report)	21. No. of Pages
NTIS	20. Security Class (This Page)	22. Price

(See ANSI-Z39.18) *See Instructions on Reverse*

OPTIONAL FORM 272 (4-77)
(Formerly NTIS-35)
Department of Commerce

CAPITAL STRATEGIES, INC.
[illegible]
KENSINGTON, MD. 20895

UNIVERSITY OF CALIFORNIA, SAN DIEGO
DEPARTMENT OF APPLIED MECHANICS AND ENGINEERING SCIENCES

LOCAL CHARACTERIZATION OF FREE-FIELD GROUND MOTION AND EFFECTS OF WAVE PASSAGE

by

J. E. Luco

and

D. A. Sotiropoulos

A Report on Research Conducted Under Grant PFR 79.00006
From the National Science Foundation

La Jolla, California

February 1980

Local Characterization of Free-Field Ground Motion and Effects of Wave Passage

by

J. E. Luco[1] and D. A. Sotiropoulos[2]

ABSTRACT

A simple model of the seismic source and of the propagation medium is used to obtain a local representation of the free-field ground motion in terms of a small number of equivalent dispersive plane waves. Numerical values for the equivalent phase velocities entering in the representation are presented for different epicentral distances and source depths. Based on the local characterization of the free-field motion, estimates of the magnitude of the effects of nonvertically incident seismic waves on the response of foundations and structures are presented.

---

[1]Assoc. Prof., Department of Applied Mechanics and Engineering Sciences, University of California, San Diego, La Jolla, California 92093.

[2]Grad. Res. Asst., Department of Applied Mechanics and Engineering Sciences, University of California, San Diego, La Jolla, California 92093.

INTRODUCTION

A number of theoretical studies (Newmark, 1969; Iguchi, 1973; Kobori and Shinozaki, 1975; Lee and Wesley, 1975; Luco, 1976a,b; Luco and Wong, 1979) have indicated the potential importance of the effects of nonvertically incident waves on the seismic response of structures. For structures supported on large continuous foundations, nonvertically incident seismic excitation may lead to filtering of the high-frequency components of the translational response and to significant torsional and rocking motions. The magnitude of the effects associated with nonvertically incident excitation depends on the assumed characterization of the seismic excitation and, in particular, on the values of the phase velocities or apparent horizontal velocities. The lower the phase velocities the more important the filtering and rotational effects. At the present time there are no experimental data which could be used to guide the selection of appropriate values for these important parameters.

The first objective of this study is to develop a simple characterization of the motion on the free-field based on a model of the seismic source and of the propagation path. The seismic source is represented as a dislocation distributed over a small area on a vertical fault plane. The propagation medium is represented as a layered elastic half-space. For this model, it is shown that the free-field motion on the ground surface can be characterized locally by a small number of "equivalent"

dispersive plane waves. The phase velocities of the "equivalent" plane waves can be calculated using the techniques available to evaluate the response of a layered half-space to a buried concentrated source (Apsel, 1979; Luco and Apsel, 1980).

The second objective of this study is to obtain estimates of the magnitude of the effects of nonvertically incident seismic waves on the response of structures supported on foundations for which embedment effects can be neglected.

A MODEL FOR THE FREE-FIELD GROUND MOTION

To obtain a representation of the free-field ground motion, it is convenient to start with a simple source model such as that illustrated in Fig. 1. In this model the seismic source is represented by a vertical fault of small area Ω located at a depth z_s from the surface of a layered elastic half-space. The horizontal (strike) and vertical (dip) slips on the plane of the fault are characterized by seismic moments $M_x(t)$ and $M_z(t)$, respectively. The plane of the fault coincides with the $x'z'$-plane in a cartesian system of coordinates (x', y', z') with origin at the epicenter and z'-axis pointing up. The Fourier Transforms of the radial, tangential and vertical components of acceleration for a point located on the ground surface at epicentral distance r and azimuth θ are denoted by $\ddot{U}_r(r, \theta, \omega)$, $\ddot{U}_\theta(r, \theta, \omega)$ and $\ddot{U}_z(r, \theta, \omega)$, respectively. These components can be written in the form

$$\begin{aligned}
\ddot{U}_r(r,\theta,\omega) &= \ddot{M}_x(\omega)\,\Sigma_{rx}(r,\omega)\sin 2\theta + \ddot{M}_z(\omega)\,\Sigma_{rz}(r,\omega)\sin\theta \\
\ddot{U}_\theta(r,\theta,\omega) &= \ddot{M}_x(\omega)\,\Sigma_{\theta x}(r,\omega)\cos 2\theta + \ddot{M}_z(\omega)\,\Sigma_{\theta z}(r,\omega)\cos\theta \qquad (1) \\
\ddot{U}_z(r,\theta,\omega) &= \ddot{M}_x(\omega)\,\Sigma_{zx}(r,\omega)\sin 2\theta + \ddot{M}_z(\omega)\,\Sigma_{zz}(r,\omega)\sin\theta
\end{aligned}$$

in which $\ddot{M}_x(\omega)$ and $\ddot{M}_z(\omega)$ represent the Fourier Transforms of the second derivatives with respect to time of the two components of the seismic moment. The functions $\Sigma_{rx}(r, \omega)\sin 2\theta$, $\Sigma_{rz}(r, \omega)\sin\theta, \ldots,$ $\Sigma_{zz}(r, \omega)\sin\theta$ correspond to the Fourier Transforms of the impulse

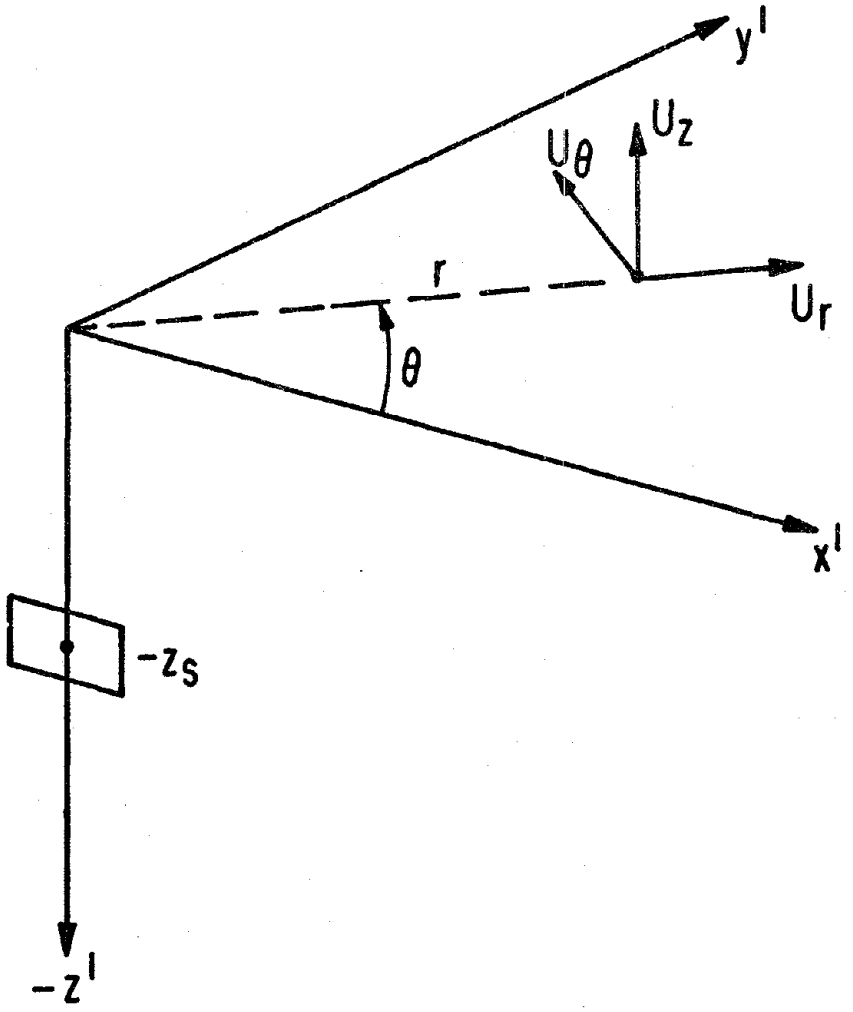

Figure 1. Description of the source-observer geometry.

response functions or Green's functions for double couples at the location of the source. The terms $\Sigma_{rx}, \Sigma_{\theta x}, \Sigma_{rz}, \ldots, \Sigma_{zz}$ depend on the geologic structure, depth of the source and epicentral distance. The representation of the free-field motion given by Eq. (1) factorizes the effects of the seismic source $[M_x(\omega), M_z(\omega)]$, propagation path $[\Sigma_{rx}(r, \omega), \Sigma_{rz}(r, \omega), \ldots]$ and radiation pattern (θ).

To arrive at a simpler characterization of the free-field motion it is necessary to analyze the properties of the Green's functions $\Sigma_{rx}, \ldots, \Sigma_{zz}$ appearing in Eq. (1) for a typical geologic structure. Of particular interest is the dependence of the Green's functions on epicentral distance. To illustrate this dependence the two geologic structures listed in Table 1 have been considered. Model 1 corresponds to the geologic structure to the southeast of Parkfield (Eaton et al., 1970), while Model 2 corresponds to the structure in the Imperial Valley (Heaton and Helmberger, 1978). The Green's functions for these geologic structures and for different source depths have been calculated by use of the method described by Apsel (1979) and Luco and Apsel (1980).

The typical effects of epicentral distance on the amplitudes of the Green's functions are shown in Figs. 2a and 2b for a frequency of 10 Hz. In Fig. 2a the amplitudes $|\Sigma_{\theta x}(r, \omega)|$, $|\Sigma_{\theta z}(r, \omega)|$ and $|\Sigma_{zx}(r, \omega)|$ are plotted versus epicentral distance for a source at a depth $z_s = 5.5$ km in Model 1. The behavior of the amplitudes $|\Sigma_{\theta x}(r, \omega)|$ and $|\Sigma_{\theta z}(r, \omega)|$ for a shallower source ($z_s = 1.0$ km, Model 1) is shown in Fig. 2b. The results presented in Figs. 2a and 2b exhibit several

TABLE 1

Characteristics of the Geologic Structures Considered

	Model 1					Model 2				
Layer No.	Depth at Bottom of Layer (km)	S-Wave Velocity (km/sec)	P-Wave Velocity (km/sec)	Density (g/cc)	$Q_S = 0.5Q_P$	Depth at Bottom of Layer (km)	S-Wave Velocity (km/sec)	P-Wave Velocity (km/sec)	Density (g/cc)	$Q_S = 0.5Q_P$
1	0.116	0.57	0.99	1.5	30	0.45	0.75	1.70	1.5	42
2	0.280	0.99	1.71	1.5	60	0.95	0.92	2.10	1.9	54
3	1.550	1.62	2.81	1.6	100	2.10	1.50	2.60	2.4	100
4	3.740	2.91	5.04	2.2	200	3.40	2.30	3.70	2.5	170
5	14.99	3.48	6.02	2.6	280	5.90	2.60	4.10	2.6	198
6	24.99	3.95	6.86	2.8	320	∞	3.70	6.40	2.8	308
7	∞	4.67	8.09	3.2	400	-	-	-	-	-

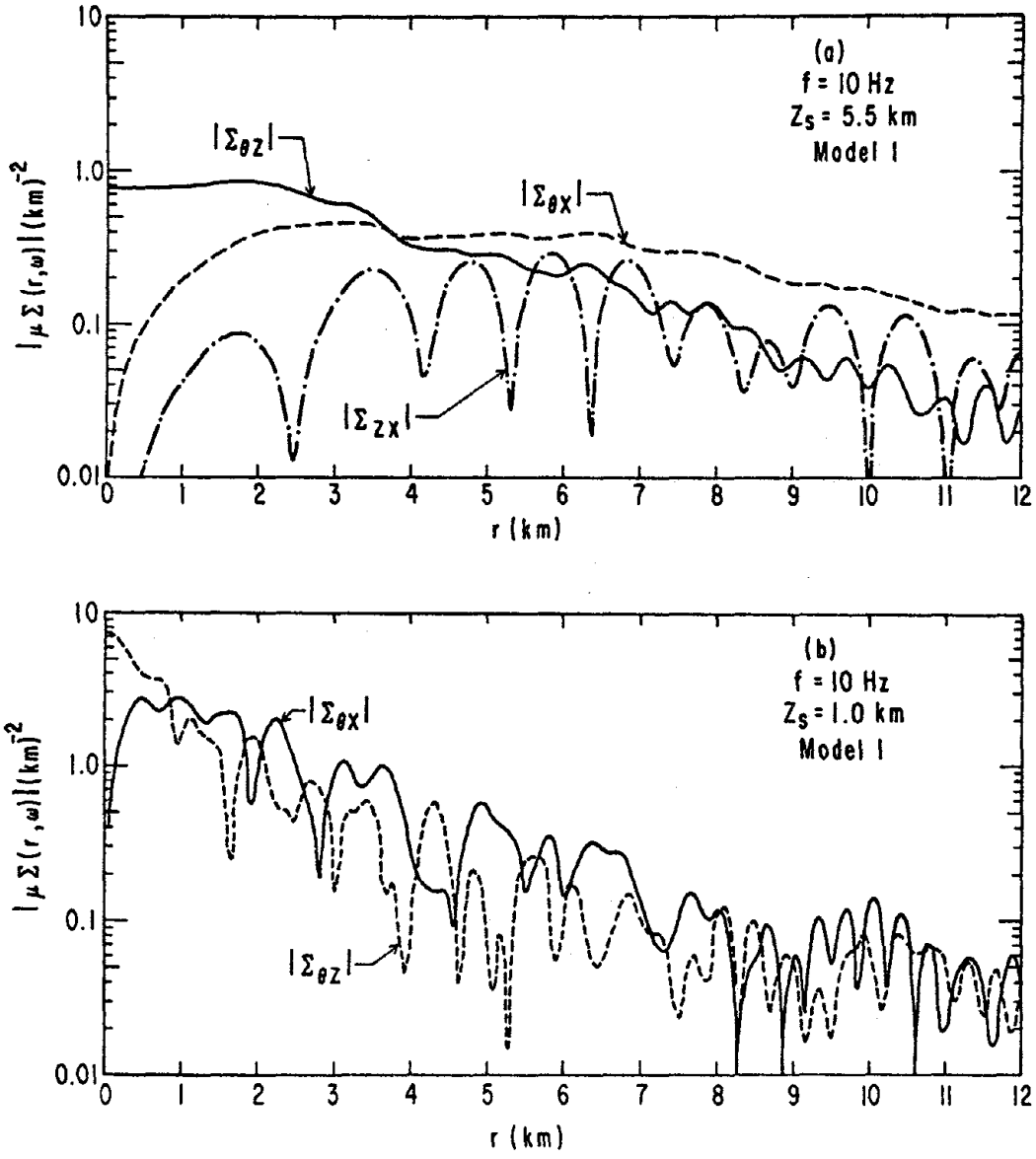

Figure 2. Dependence of the amplitudes of the Green's functions on epicentral distance for a frequency of 10 Hz: (a) source depth 5.5 km, (b) source depth 1.0 km. The geologic structure corresponds to Model 1 listed in Table 1. (μ = shear modulus at source depth)

interesting characteristics. For epicentral distances larger than a few kilometers a general reduction in amplitude with epicentral distance can be observed. This reduction is associated with geometrical spreading and material attenuation. The attenuation is somewhat more pronounced for the shallower source (Fig. 2b). A second observation is that as epicentral distance tends to zero the amplitudes of the Green's functions associated with strike-slip dislocation (Σ_{rx}, $\Sigma_{\theta x}$, Σ_{zx}) also tend to zero. On the other hand, of the Green's functions associated with dip-slip dislocation, Σ_{rz} and $\Sigma_{\theta z}$ tend to a finite value while Σ_{zz} tends to zero as epicentral distance tends to zero. The most striking feature of the results presented corresponds to the strong fluctuations in amplitude with epicentral distance for a shallow source (Fig. 2b). For a deep source (Fig. 2a) the amplitudes of the Green's functions associated with the vertical components of motion (Σ_{zx}, Σ_{zz}) continue to exhibit these fluctuations while the amplitudes of the Green's functions associated with horizontal components of motion (Σ_{rz}, $\Sigma_{\theta x}$, Σ_{rz}, $\Sigma_{\theta z}$) are smoother functions of epicentral distance. In general, the dependence of the Green's functions on epicentral distance increases with frequency.

Despite the strong dependence on epicentral distance exhibited in Figs. 2a and 2b, it is possible to assume, as a first approximation, that the amplitudes of the Green's functions remain unchanged for variations in epicentral distance of the order of a few tens of meters.

The typical dependence of the phase angle of the Green's functions on epicentral distance is illustrated in Fig. 3. In this figure, the phase

angle $\phi_{\theta x}(r, \omega)$ of the Green's function $\Sigma_{\theta x} = |\Sigma_{\theta x}| \exp(i\phi_{\theta x})$ for a source at a depth of 5.5 km is shown versus epicentral distance for a frequency of 10 Hz (Model 1). It is apparent from Fig. 3 that the phase angle changes rapidly with epicentral distance and that for small variations in epicentral distance the corresponding variation in phase angle can be assumed to be linear.

Based on the discussion above it is possible to write

$$\Sigma_{\alpha\beta}(r, \omega) \approx \Sigma_{\alpha\beta}(r_o, \omega) \exp[-i\omega(r - r_o)/c_{\alpha\beta}(r_o, \omega)] \tag{2}$$

for $|r - r_o|$ less than a few tens of meters. In Eq. (2) the subscript α stands for r, θ or z, while the subscript β stands for x or z. The quantities $c_{\alpha\beta}(r_o, \omega)$ are defined by

$$\frac{1}{c_{\alpha\beta}(r_o, \omega)} = -\frac{1}{\omega} \left(\frac{d\phi_{\alpha\beta}}{dr}\right)_{r = r_o} \tag{3}$$

and correspond to frequency-dependent phase velocities. These equivalent phase velocities are not associated with a particular type of wave but rather reflect the characteristics of the total motion in a given direction for a given epicentral distance and frequency.

Equations (1) and (2) indicate that the free-field motion in the vicinity of a point on the ground surface can be approximately represented by a superposition of six dispersive plane waves. This approximation rests on the assumption of a small seismic source on a vertical

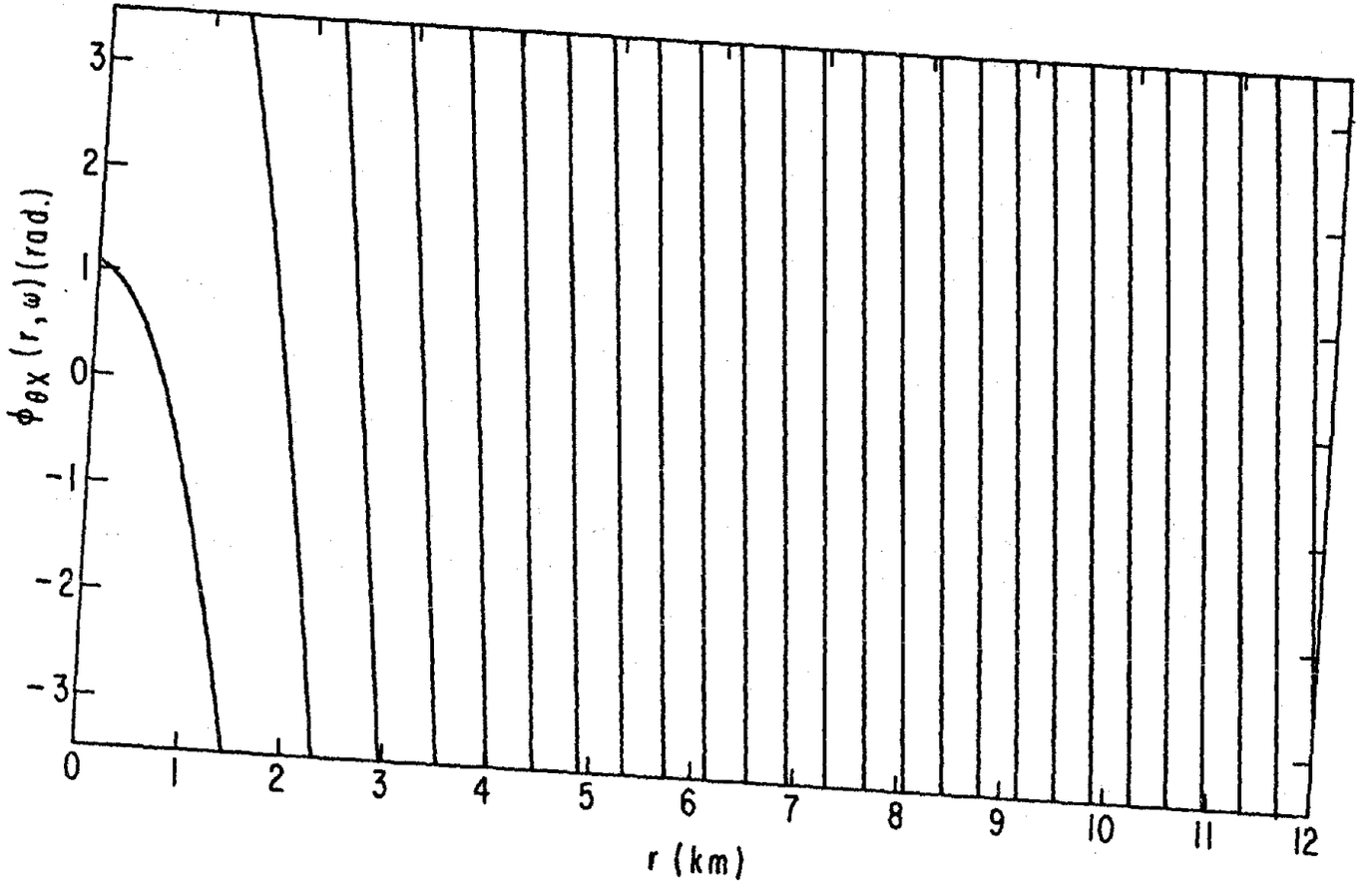

Figure 3. Dependence of the phase $\phi_{\theta x}$ of the Green's function $\Sigma_{\theta x}$ on epicentral distance for a frequency of 10 Hz. The source is at a depth of 5.5 km in the geologic structure corresponding to Model 1.

fault plane. The finite number of equivalent plane waves represent the more complex superposition of waves arriving at a site.

The equivalent phase velocities $c_{rx}, \ldots, c_{zz}$ play a key role in the local characterization of the free-field motion. The reciprocals of the phase velocities $c_{\theta x}(r,\omega)$, $c_{rx}(r,\omega)$ and $c_{zx}(r,\omega)$ for strike-slip dislocation are shown in Fig. 4 versus epicentral distance r for frequencies of 1, 5.5 and 10 Hz. The source considered is at a depth of 5.5 km in the geologic structure corresponding to Model 1. The reciprocals of the corresponding phase velocities for dip-slip dislocation are shown in Fig. 5. The results presented in Figs. 4 and 5 indicate that for epicentral distances less than the source depth, the phase velocities are high and essentially independent of frequency, in agreement with the physical expectation of a dominant direct ray in this region. For epicentral distances in the range from 5 to 12 km the phase velocities exhibit a dependence on both frequency and epicentral distance. In this range of epicentral distances, the phase velocities $c_{\theta x}$, $c_{\theta z}$, c_{rz} and c_{zz} oscillate about a value of the order of 3.5 km/sec, while c_{rx} and c_{zx} oscillate about a value of approximately 5.0 km/sec.

For shallower sources, the dependence of the phase velocities on frequency and epicentral distance is more pronounced due to multiple reflections in the surface layers as illustrated in Fig. 6. In this figure, the reciprocal of the phase velocity $c_{\theta x}$ is shown versus epicentral distance for a source at a depth $z_s = 1.0$ km in Model 1. For epicentral distances in the range from 1 to 12 km the phase velocity $c_{\theta x}$ oscillates about a value of the order of 1.8 km/sec.

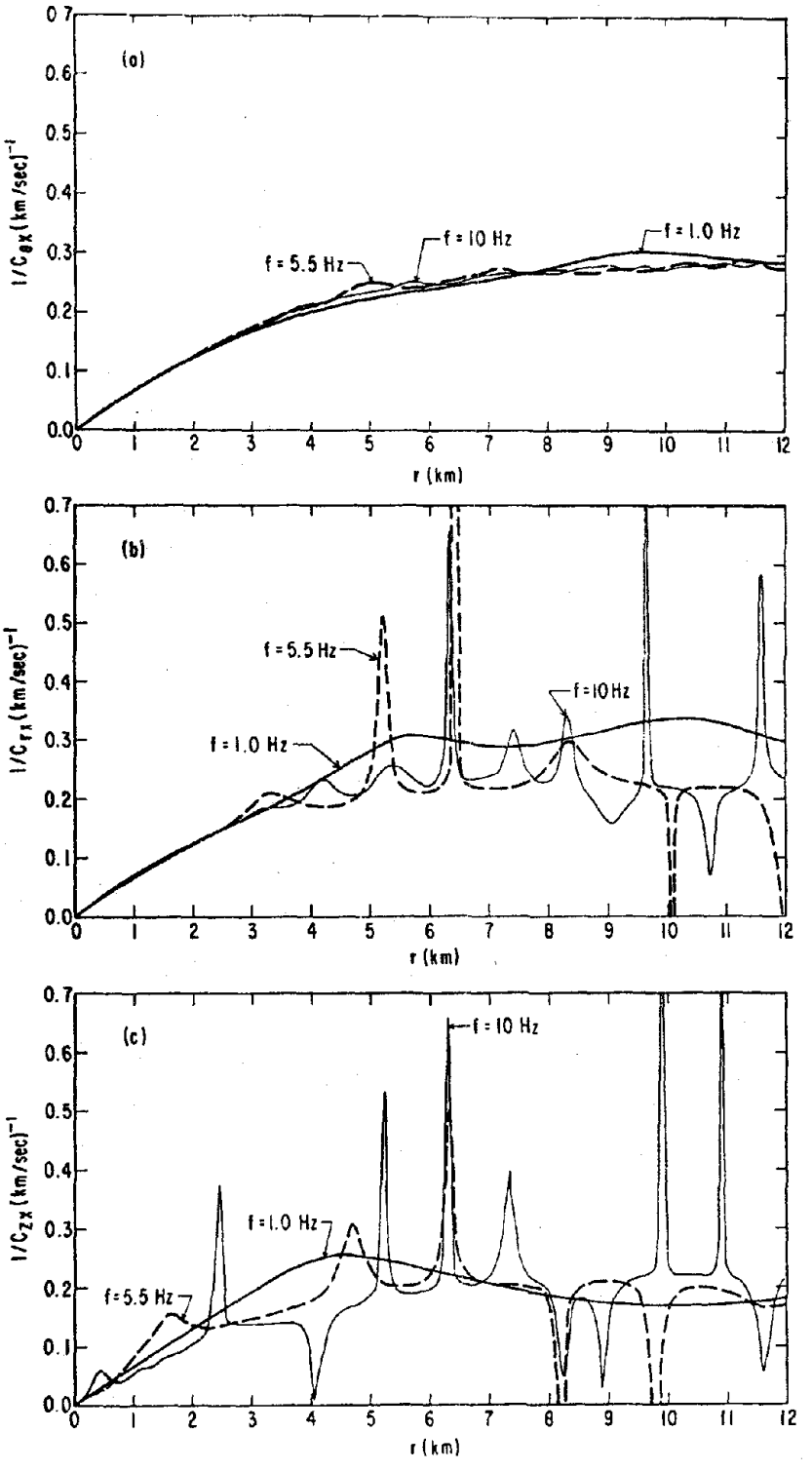

Figure 4. Dependence of the equivalent phase velocities $c_{\theta x}$, c_{rx} and c_{zx} on epicentral distance for frequencies of 1.0, 5.5 and 10 Hz. The source is at a depth of 5.5 km in the geologic structure corresponding to Model 1.

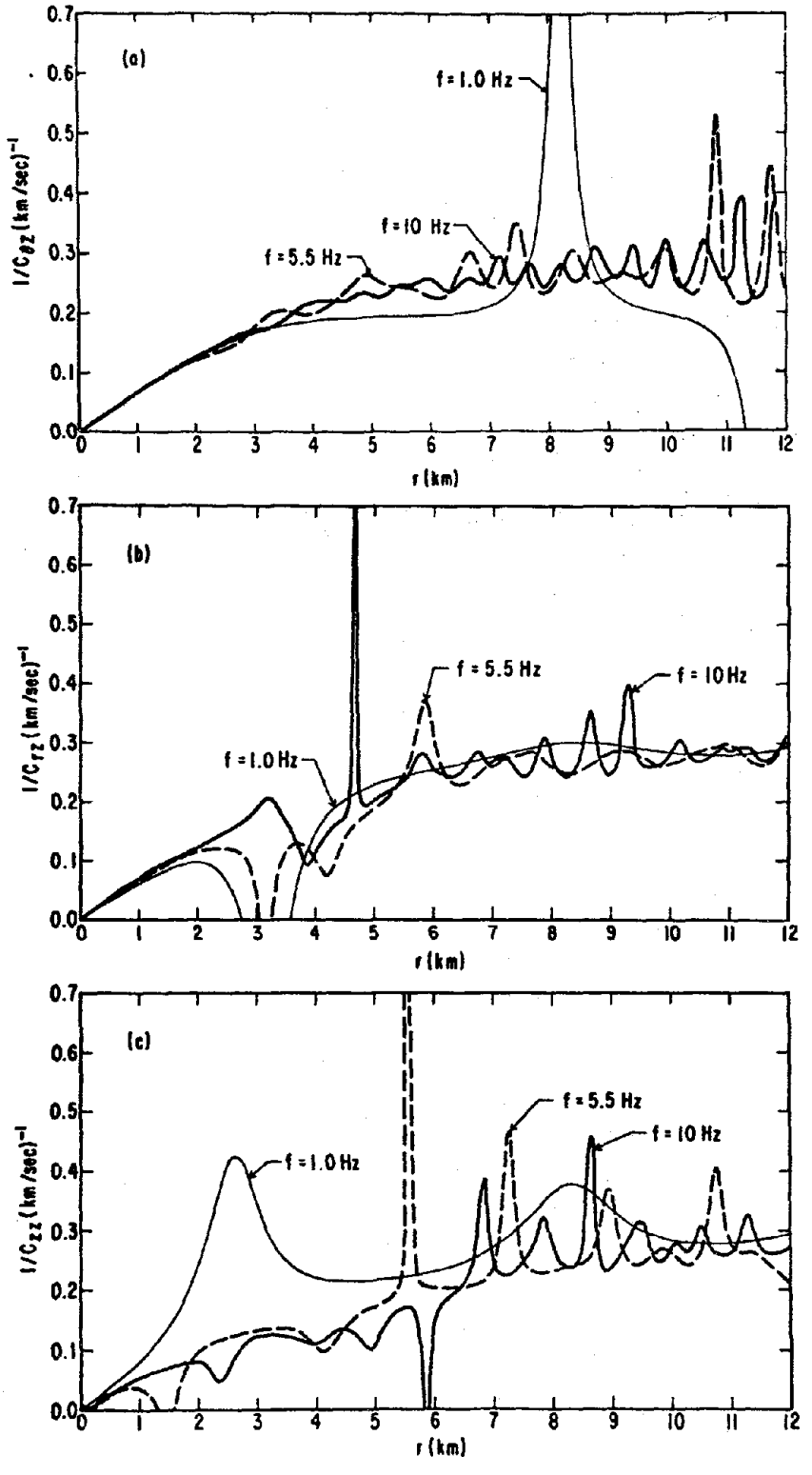

Figure 5. Dependence of the equivalent phase velocities $c_{\theta z}$, c_{rz} and c_{zz} on epicentral distance for frequencies of 1.0, 5.5 and 10 Hz (z_s = 5.5 km, Model 1).

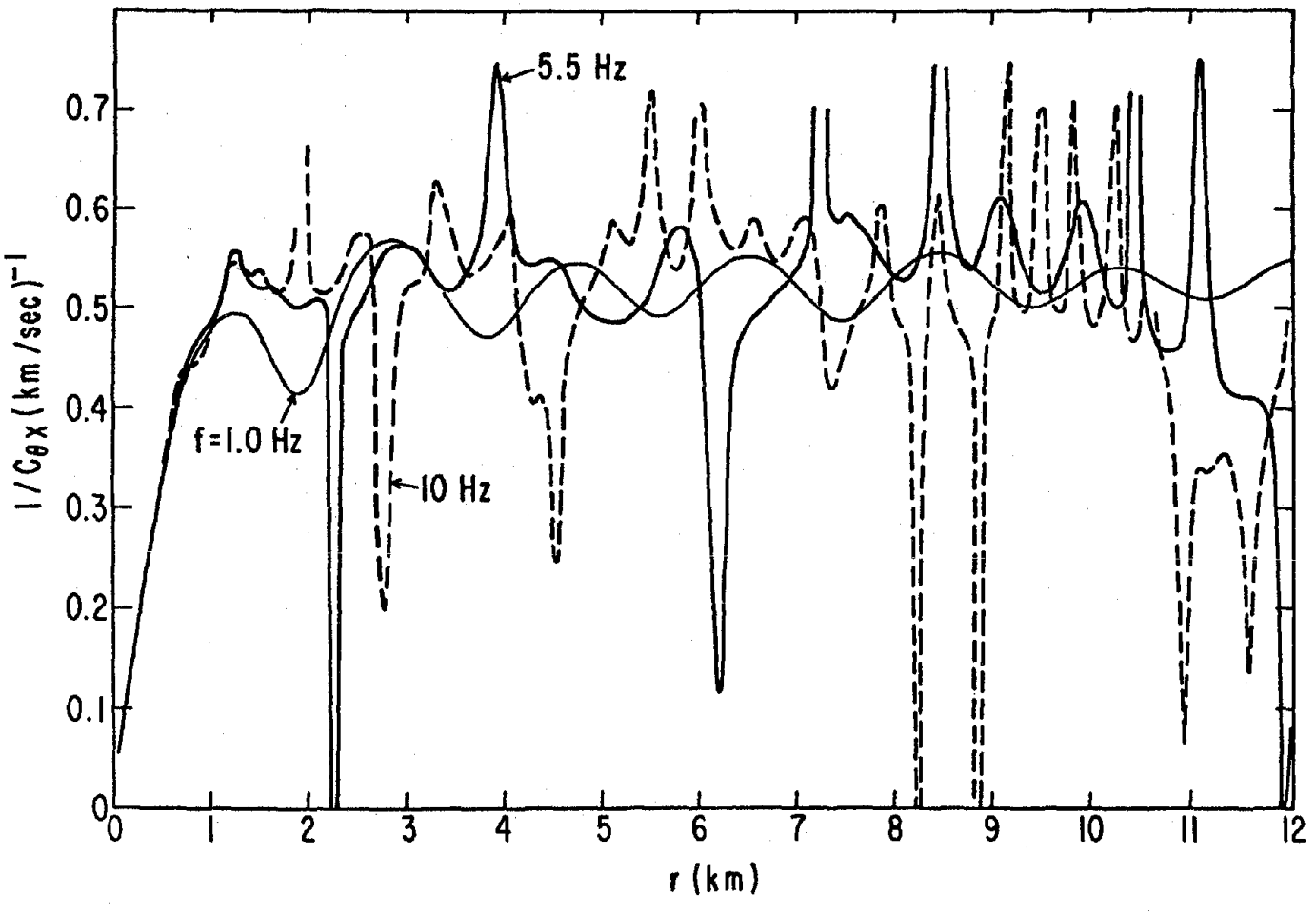

Figure 6. Dependence of the equivalent phase velocity $c_{\theta x}$ on epicentral distance for frequencies of 1.0, 5.5 and 10 Hz. The source is at a depth of 1.0 km in the geologic structure corresponding to Model 1.

To obtain estimates of the effects of wave passage on extended foundations it is convenient to simplify the representation of the free-field motion even further. This is accomplished by considering only two phase velocities defined by

$$c_H = c_{\theta x} \quad , \quad c_V = c_{zx} \approx c_{rx} \tag{4}$$

for the case in which strike-slip dislocation is predominant and by

$$c_H = c_{\theta z} \quad , \quad c_V = c_{zz} \approx c_{rz} \tag{5}$$

for predominant dip-slip dislocation. The phase velocity $c_H(r, \omega)$ characterizes the tangential component of motion, while the radial and vertical components are characterized by a common phase velocity $c_V(r, \omega)$. By use of Eqs. (1), (2), and (4) or (5) it is found that

$$\begin{aligned}
\ddot{U}_\theta(r, \theta, \omega) &\approx \ddot{U}_\theta(r_o, \theta_o, \omega) \exp[-i\omega(r - r_o)/c_H(r_o, \omega)] \\
\ddot{U}_r(r, \theta, \omega) &\approx \ddot{U}_r(r_o, \theta_o, \omega) \exp[-i\omega(r - r_o)/c_V(r_o, \omega)] \\
\ddot{U}_z(r, \theta, \omega) &\approx \ddot{U}_z(r_o, \theta_o, \omega) \exp[-i\omega(r - r_o)/c_V(r_o, \omega)]
\end{aligned} \tag{6}$$

for $|r - r_o|$ less than a few tens of meters and $|\theta - \theta_o| \ll 1^o$.

The representation given by Eq. (6) indicates that the free-field motion in the neighborhood of a point with cylindrical coordinates $(r_o, \theta_o, 0)$ can be approximately obtained if the motion at that point and the equivalent phase velocities $c_H(r_o, \omega)$ and $c_V(r_o, \omega)$ are known. Since considerable strong motion data are available, the frequency content of the motion at a point can be estimated for a given magnitude,

epicentral distance and type of soil condition (Trifunac, 1976; McGuire, 1978). As illustrated above, given the geologic structure and the epicentral distance it is also possible to estimate the equivalent phase velocities c_H and c_V. The representation given by Eq. (6) circumvents a more complex decomposition of the free-field motion involving different types of waves each characterized by its own frequency content and phase velocity.

For structures supported on embedded foundations it is also necessary to describe the free-field motion at depth. The tangential components of the free-field motion at depth can be obtained by considering plane SH-waves with phase velocity c_H and total amplitude $\ddot{U}_\theta$ on the ground surface. Similarly, the radial and vertical components of motion can be represented by a consideration of plane P- and SV-waves with common phase velocity c_V and amplitudes $\ddot{U}_r$ and $\ddot{U}_z$ on the ground surface.

FOUNDATION INPUT MOTION

To estimate the effects of wave passage a rigid massless rectangular foundation is considered. The foundation is centered at a point 0 located at epicentral distance r_o in the azimuth θ_o from the strike of the fault (Fig. 7). A local cartesian system of coordinates (x, y, z) with origin at the center of the foundation and with x- and y-axes in the directions of the axes of symmetry of the foundation is employed. The x-axis forms the angle θ_H with the line connecting the epicenter and the center of the foundation. Referred to the local system of coordinates the foundation occupies the region ($|x| \leq a$, $|y| \leq b$, $z = 0$). The free-field motion given by Eq. (6) when expressed in the local system of coordinates can be written in the form

$$\begin{Bmatrix} \ddot{U}_x(x,y,\omega) \\ \ddot{U}_z(x,y,\omega) \\ \ddot{U}_z(x,y,\omega) \end{Bmatrix} = \begin{Bmatrix} \ddot{U}_{rg} \cos\theta_H \\ \ddot{U}_{rg} \sin\theta_H \\ \ddot{U}_{zg} \end{Bmatrix} \exp\left[-\frac{i\omega(r-r_o)}{c_V}\right] + \begin{Bmatrix} -\ddot{U}_{\theta g} \sin\theta_H \\ \ddot{U}_{\theta g} \cos\theta_H \\ 0 \end{Bmatrix} \exp\left[-\frac{i\omega(r-r_o)}{c_H}\right] \tag{7}$$

where $\ddot{U}_{rg}$, $\ddot{U}_{\theta g}$ and $\ddot{U}_{zg}$ represent the Fourier-Transforms of the radial, tangential and vertical components of the free-field motion at the center of the foundation. In Eq. (7) the term $(r - r_o)$ can be approximated by $r - r_o \approx x \cos\theta_H + y \sin\theta_H$.

The response of the rigid massless foundation to the free-field motion given by Eq. (7) can be described by the translational response

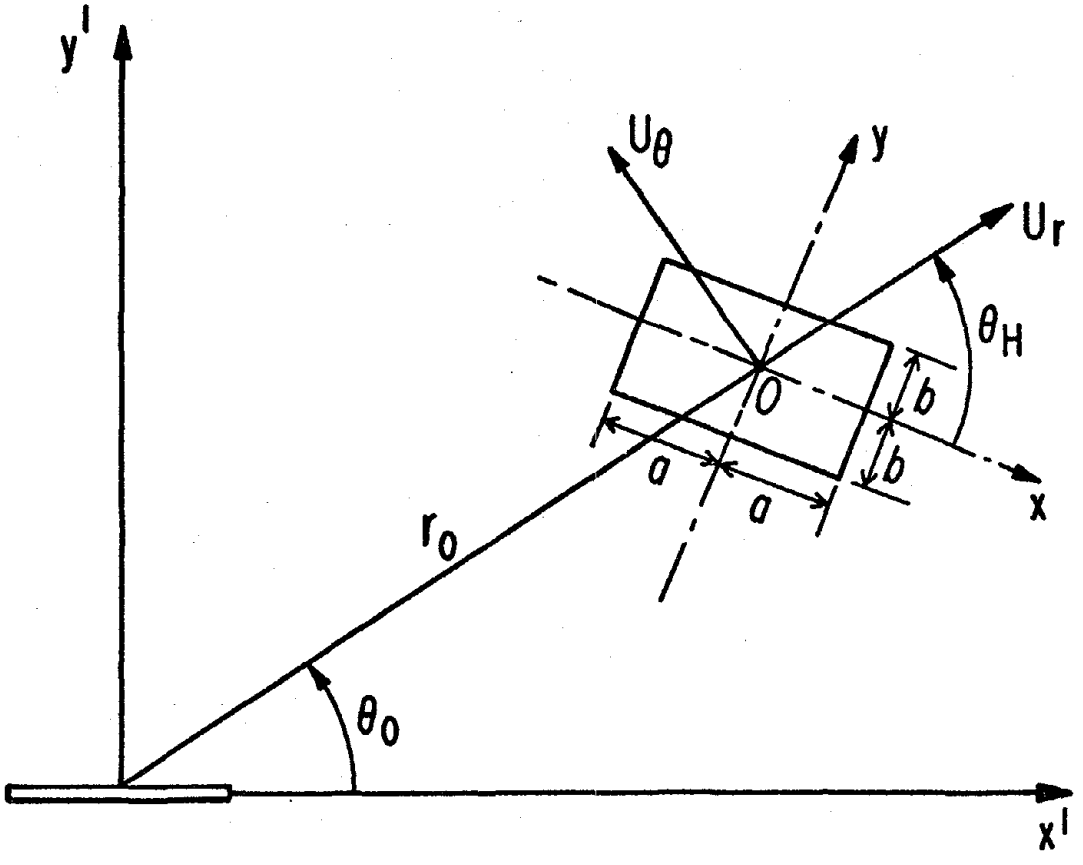

Figure 7. Geometry of the foundation with respect to the seismic source.

at the center of the foundation $[\ddot{U}^*_{xo}(\omega),\ \ddot{Y}^*_{yo}(\omega),\ \ddot{U}^*_{zo}(\omega)]$ and by the rotation vector $[\ddot{\phi}^*_{xo}(\omega),\ \ddot{\phi}^*_{yo}(\omega),\ \ddot{\phi}^*_{zo}(\omega)]$. The vector

$$\{\ddot{U}^*_o\} = (\ddot{U}^*_{xo},\ \ddot{U}^*_{yo},\ U^*_{zo},\ \ddot{\phi}^*_{xo},\ \ddot{\phi}^*_{yo},\ \ddot{\phi}^*_{zo})^T\ , \tag{8}$$

designated as foundation input motion, plays a key role in determining the seismic response of structures. The total response at foundation level $\{\ddot{U}_o(\omega)\}$, including translations and rotations, after the effects of soil-structure interaction have been considered, can be written in the form

$$\{\ddot{U}_o\} = \left([I] - \omega^2[C(\omega)]([M_o] + [M_b(\omega)])\right)^{-1}\{\ddot{U}^*_o\} \tag{9}$$

where $[I]$ is the 6×6 identity matrix, $[C(\omega)]$ is the compliance matrix for the foundation, $[M_o]$ is the mass matrix for the foundation and $[M_b(\omega)]$ is the equivalent frequency-dependent mass matrix for the superstructure (Wong and Luco, 1978a; Luco and Wong, 1979). Once the total response $\{\ddot{U}_o(\omega)\}$ of the foundation has been obtained, the response at any point in the superstructure can be determined by standard methods. Equation (9) indicates that for a complete study of the effects of wave passage it is necessary to consider the properties of the superstructure. Valuable information, independent of the structural configuration, can be gained however by examining the characteristics of the foundation input motion $\{\ddot{U}^*_o\}$.

Accurate methods to evaluate the response of rigid foundations to a free-field motion of the type described by Eq. (7) are available (Wong and Luco, 1978a, b). To obtain estimates of the foundation input motion it is sufficient, however, to use the approximate averaging procedure discussed by Tani et al. (1973), Iguchi (1973) and Scanlan (1976). The resulting estimates are:

$$\begin{Bmatrix} \ddot{U}^{*}_{xo}(\omega) \\ \ddot{U}^{*}_{yo}(\omega) \\ \ddot{U}^{*}_{zo}(\omega) \end{Bmatrix} = \left(\frac{\sin a_v}{a_v}\right)\left(\frac{\sin b_v}{b_v}\right)\begin{Bmatrix} \ddot{U}_{rg}(\omega)\cos\theta_H \\ \ddot{U}_{rg}(\omega)\sin\theta_H \\ \ddot{U}_{zg}(\omega) \end{Bmatrix} + \left(\frac{\sin a_H}{a_H}\right)\left(\frac{\sin b_H}{b_H}\right)\begin{Bmatrix} -\ddot{U}_{\theta g}(\omega)\sin\theta_H \\ \ddot{U}_{\theta g}(\omega)\cos\theta_H \\ 0 \end{Bmatrix} \tag{10}$$

$$\frac{a\,\ddot{\phi}^{*}_{yo}(\omega)}{\ddot{U}_{zg}(\omega)} = i\,\frac{3}{a_v}\left(\frac{\sin a_v}{a_v} - \cos a_v\right)\frac{\sin b_v}{b_v} \tag{11}$$

$$\frac{b\,\ddot{\phi}^{*}_{xo}(\omega)}{\ddot{U}_{zg}(\omega)} = i\,\frac{-3}{b_v}\left(\frac{\sin b_v}{b_v} - \cos b_v\right)\frac{\sin a_v}{a_v} \tag{12}$$

$$\begin{aligned} \ddot{\phi}^{*}_{zo}(\omega) = -\frac{3i}{a^2+b^2}\Bigg[&\left(\frac{\sin a_H}{a_H^2} - \frac{\cos a_H}{a_H}\right)\frac{\sin b_H}{b_H}\,a\,\ddot{U}_{\theta g}(\omega)\cos\theta_H \\ &+ \left(\frac{\sin b_H}{b_H^2} - \frac{\cos b_H}{b_H}\right)\frac{\sin a_H}{a_H}\,b\,\ddot{U}_{\theta g}(\omega)\sin\theta_H \\ &+ \left(\frac{\sin a_v}{a_v^2} - \frac{\cos a_v}{a_v}\right)\frac{\sin b_v}{b_v}\,a\,\ddot{U}_{rg}(\omega)\sin\theta_N \\ &- \left(\frac{\sin b_v}{b_v^2} - \frac{\cos b_b}{b_v}\right)\frac{\sin a_v}{a_v}\,b\,\ddot{U}_{rg}(\omega)\cos\theta_H\Bigg] \end{aligned} \tag{13}$$

where

$$a_H = (\omega a/c_H)\cos\theta_H \quad , \quad b_H = (\omega b/c_H)\sin\theta_H$$
$$a_v = (\omega a/c_V)\cos\theta_H \quad , \quad b_v = (\omega b/c_V)\sin\theta_H \tag{14}$$

In the particular case of a foundation oriented such that $\theta_H = 0$ then

$$\ddot{U}_{rg}(\omega) = \ddot{U}_{xg}(\omega) \quad , \quad \ddot{U}_{\theta g}(\omega) = \ddot{U}_{yg}(\omega) \tag{15}$$

and the above estimates of the foundation input motion reduce to

$$\frac{\ddot{U}^*_{yo}(\omega)}{\ddot{U}_{yg}(\omega)} = \frac{\sin \hat{a}_H}{\hat{a}_H} \tag{16}$$

$$\frac{\ddot{U}^*_{xo}(\omega)}{\ddot{U}_{xg}(\omega)} = \frac{\ddot{U}^*_{zo}(\omega)}{\ddot{U}_{zg}(\omega)} = \frac{\sin \hat{a}_v}{\hat{a}_v} \tag{17}$$

$$\frac{a\ddot{\phi}^*_{yo}(\omega)}{\ddot{U}_{zg}(\omega)} = \frac{3i}{\hat{a}_v}\left(\frac{\sin \hat{a}_v}{\hat{a}_v} - \cos \hat{a}_v\right) \tag{18}$$

$$\frac{b\ddot{\phi}^*_{xo}(\omega)}{\ddot{U}_{zg}(\omega)} \approx 0 \tag{19}$$

$$\frac{a\ddot{\phi}^*_{zo}(\omega)}{\ddot{U}_{yg}(\omega)} = \frac{-3i}{[1+(b/a)^2]\,\hat{a}_H}\left(\frac{\sin \hat{a}_H}{\hat{a}_H} - \cos \hat{a}_H\right) \tag{20}$$

where $\hat{a}_H = \omega a/c_H$ and $\hat{a}_v = \omega a/c_V$. For small values of $\hat{a}_H$ and $\hat{a}_v$, the right hand sides of Eqs. (18) and (20) reduce to $i\hat{a}_v$ and $-i\hat{a}_H/[1+(b/a)^2]$, respectively. The estimates of the foundation input motion given by Eqs. (16) - (20) will be used to evaluate the effects of wave passage. In these calculations, the phase velocities c_H and c_V will be taken to correspond to $c_{\theta x}$ and c_{zx}, respectively.

EFFECTS OF WAVE PASSAGE ON THE HORIZONTAL AND TORSIONAL RESPONSE

The effects of wave passage on the horizontal and torsional response of a square foundation of half-width a = b = 20 m are illustrated in Fig. 8. In this figure the amplitude ratios $|\ddot{U}^*_{yo}/\ddot{U}_{yg}|$ and $|a\ddot{\phi}_{zo}/\ddot{U}_{yg}|$ are shown versus frequency for epicentral distances of 1, 10 and 50 km (Figs. 8a, b and c, respectively). The seismic sources are assumed to be located in the geologic structure corresponding to Model 1 at depths of 1 and 5.5 km. For comparison, the corresponding results for a different geologic structure (Model 2, Table 1) are shown in Fig. 8d for an epicentral distance r = 10 km. The results shown in Fig. 8 indicate that the dependence on source depth tends to decrease as epicentral distance increases. For Model 1, the effects of wave passage become approximately independent of source depth at an epicentral distance of the order of 20 km (for sources at depths shallower than 20 km).

In general, the effects of wave passage on the horizontal response at the center of the foundation ($\ddot{U}^*_{yo}$) are small. For a source at a depth of 5.5 km and a frequency of 10 Hz, the reductions of the translational motion of the foundation (a = 20 m) with respect to the free-field motion are 0.1, 2 and 1.5 percent for epicentral distances of 1, 10 and 50 km, respectively. The corresponding reductions for a frequency of 20 Hz are 0.5, 8 and 6 percent. The filtering effects could become relatively more important at very short epicentral distances and extremely

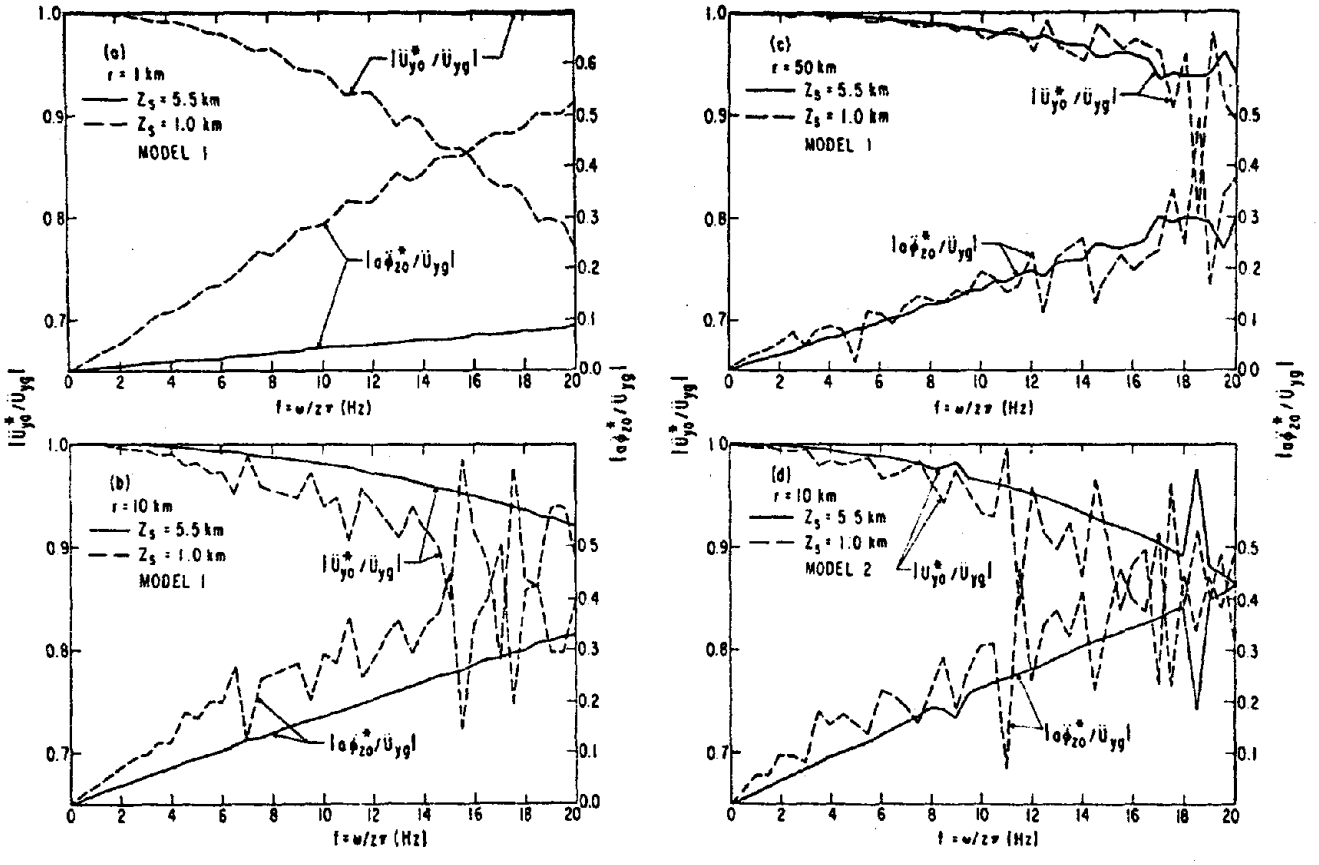

Figure 8. Effects of wave passage on the horizontal (ordinates on the left) and torsional (ordinates on the right) response of a massless rectangular foundation of half-width a = b = 20 m. Figures (a), (b) and (c) correspond to geologic model 1 and to epicentral distances r = 1, 10 and 50 km, respectively. Figure (d) corresponds to geologic model 2 and epicentral distance r = 10 km.

shallow sources as shown in Fig. 8a, or, in the case of extremely large foundations. For an extended foundation of half-width a = 50 m in the direction of propagation of the seismic waves, the reductions at 10 and 20 Hz would be of the order of 10 and 40 percent, respectively (r = 1 km, z_s = 1 km).

The torsional response of the foundation is such that the tangential component of motion on the perimeter of the foundation $a\ddot{\phi}^*_{zo}(\omega)$ associated with torsion can amount to a significant percentage of the free-field motion amplitude $\ddot{U}_{yg}(\omega)$. For a source at a depth of 5.5 km and a frequency of 10 Hz the results shown in Fig. 8 indicate that the tangential motion on the perimeter amounts to 4.5, 17 and 16 percent of the free-field motion for epicentral distances of 1, 10 and 50 km, respectively. For shallower sources and short epicentral distances the tangential motion at 10 Hz could be as high as 29 percent of the free-field motion for a square foundation of half-width a = 20 m (Fig. 8a).

The Uniform Building Code requires as minimum an accidental eccentricity of 5 percent of the larger plan dimension to cover in part for the torsional effects introduced by nonvertically incident seismic waves. The adequacy of this requirement can be studied by referring to the work of Newmark (1969) in which equivalent eccentricities necessary to account for possible torsional excitation are derived.

According to Newmark (1969), the equivalent accidental eccentricity e_x for buildings structured with shear walls along the perimeter ($a \geq b$) is

given by

$$e_x/2a = \alpha[1 + (b/a)]f_y t_a \tag{21}$$

in which f_y is the fundamental frequency for vibrations in the y-direction, $\alpha = 1.25$ for $0.3 \leq f_y < 1.0$, and $\alpha = 0.75$ for $1.5 \leq f_y \leq 5.0$. The term t_a is defined by

$$t_a = \frac{2a\phi^*_{zmax}}{\dot{U}_{ygmax}} \tag{22}$$

where ϕ^*_{zmax} is the peak value of the torsional rotation of the base and $\dot{U}_{ygmax}$ is the peak velocity of the free-field motion in the direction normal to the longer plan dimension.

The results shown in Fig. 8 and Eq. (20) indicate that $a\ddot{\phi}^*_{zo}(\omega)/\ddot{U}_{yg}(\omega)$ can be approximated by

$$a\ddot{\phi}^*_{zo}(\omega)/\ddot{U}_{yg}(\omega) \approx -i(\omega a/c_H)/[1 + (b/a)^2] \tag{23}$$

and, consequently

$$\phi^*_{zmax}/\dot{U}_{ygmax} = \{c_H[1 + (b/a)^2]\}^{-1} \quad . \tag{24}$$

From Eqs. (22) and (24) it is found that

$$t_a = 2a/\{c_H[1 + (b/a)^2]\} \quad . \tag{25}$$

This expression for t_a incorporates the aspect ratio of the foundation and differs from the expression used by Newmark ($t_a = 2a/c_H$) .

Substitution from Eq. (25) into Eq. (21) leads to

$$e_x/2a = 2\alpha \left[\frac{1 + (b/a)}{1 + (b/a)^2}\right]\left(\frac{f_y a}{c_H}\right) \quad . \tag{26}$$

This expression can be used to calculate the equivalent 'accidental' eccentricity after an estimate of the equivalent phase velocity c_H has been obtained. An alternative form can be obtained by use of Eqs. (23) and (26). The resulting expression is

$$e_x/2a \approx \frac{2\alpha}{\pi}\left(\frac{a}{20}\right)\left[\frac{1 + (b/a)}{1 + (b/a)^2}\right]\left|\frac{a\ddot{\phi}^*_{zo}(\omega_y)}{\ddot{U}_{yg}(\omega_y)}\right|_{a = b = 20\ m} \tag{27}$$

where a is in meters and $\omega_y = 2\pi f_y$. Numerical values for the last factor appearing in Eq. (27) are shown versus frequency in Fig. 8.

Based on Eq. (27) and on the results shown in Fig. 8 it is possible to estimate the equivalent accidental eccentricities for different structures and different epicentral distances. For example, the equivalent accidental eccentricity for a symmetric structure with $f_y = 5$ Hz and $a = b = 20$ m located at an epicentral distance of 10 km from a source at a depth of 5.5 km (Model 1) would be $e_x/2a = 0.053$. Finally, in the unlikely situation of an epicentral distance of 1 km and a shallow source at a depth of 1 km the equivalent eccentricity would be $e_x/2a = 0.07$. It seems, then, that an accidental eccentricity of 5 percent is sufficient to cover for the effects of wave passage for structures with fundamental frequencies lower than 5 Hz and foundation lengths in the direction of propagation (2a) less than 40 meters.

EFFECTS OF WAVE PASSAGE ON THE VERTICAL AND ROCKING RESPONSE

The effects of wave passage on the vertical and rocking response of a rectangular foundation of half-width a = 20 in the direction of propagation are illustrated in Fig. 9. In particular, the amplitude ratios $|\ddot{U}^*_{zo}/\ddot{U}_{zg}|$ and $|a\ddot{\phi}^*_{yo}/\ddot{U}_{zg}|$ are shown versus frequency in Figs. 9a, b and c for epicentral distances r = 1, 10 and 50 km, respectively. The results presented correspond to sources located at depths of 1 and 5.5 km in the geologic structure described by Model 1. The results shown in Fig. 9 indicate that the vertical response of the foundation, $\ddot{U}^*_{zo}(\omega)$ is only slightly lower than the vertical component of the free-field motion, $\ddot{U}_{zg}(\omega)$. For a source at a 5.5 km depth the reductions associated with filtering amount to less than 5 percent. Slightly higher reductions are obtained for a shallow source (z_s = 1.0 km) at epicentral distances shorter than 10 km. For very short epicentral distances and very shallow sources (r = 1 km, z_s = 1 km) the reductions are of the order of 15 percent at 20 Hz. The effects of wave passage on the $\ddot{U}_{xo}$ component of motion are equal to those for the vertical component as indicated by Eq. (17).

The vertical component of the free-field motion, $\ddot{U}_{zg}(\omega)$, induces a small but still significant rocking component of motion, $\ddot{\phi}^*_{yo}(\omega)$. As illustration, at a frequency of 20 Hz and for a foundation of half-width a = 20 m, the vertical motion induced by rocking on the perimeter of the foundation, $a\ddot{\phi}^*_{yo}$, amounts to 40 percent of the vertical motion in the free-field (r = 10 - 50 km, z_s = 5.5 km). Larger rocking components are

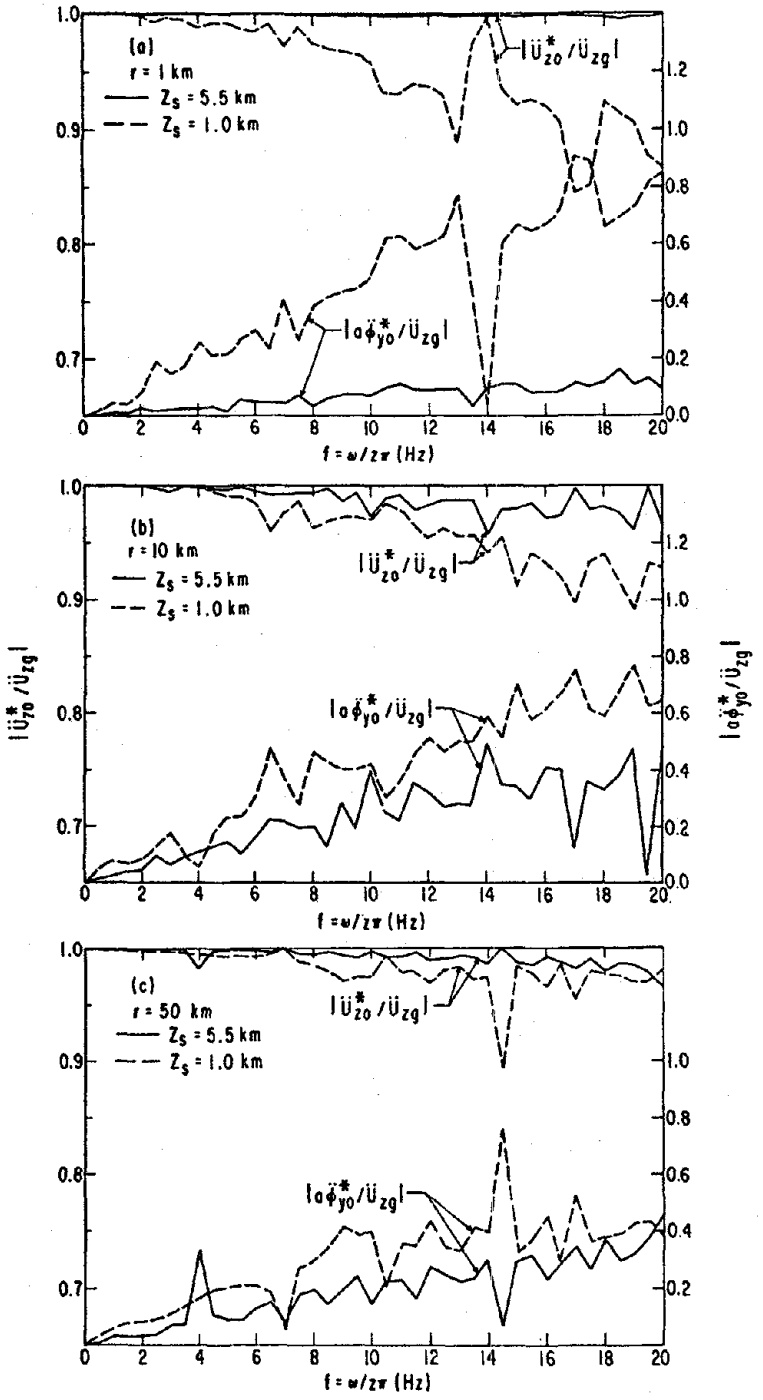

Figure 9. Effects of wave passage on the vertical (ordinates on the left) and rocking (ordinates on the right) response of a massless square foundation of half-width a = b = 20 m. Figures (a), (b) and (c) correspond to geologic model 1 and to epicentral distances r = 1, 10 and 50 km, respectively.

induced by extremely shallow sources ($z_s \sim 1$ km) at short epicentral distances ($r \sim 1 - 10$ km) as shown in Figs. 9a and b.

To estimate the effects of rocking of the foundation on the structural response it is convenient to recall that the contribution of the first mode to the relative horizontal displacement of a superstructure subjected to translation $\ddot{U}_{xo}(\omega)$ and rocking $\ddot{\phi}_{yo}(\omega)$ of its base is proportional to the function

$$\kappa_1(\omega) = \beta_1 [\, \ddot{U}_{xo}(\omega) + \gamma_1 H \ddot{\phi}_{yo}(\omega)] \tag{28}$$

where H is the height of the structure, β_1 is the participation factor and γ_1 is a modal parameter that in most cases has a value of approximately 0.7. The contribution of the first mode to the base shear force and overturning moment is also proportional to κ_1. If the effects of soil-structure interaction are neglected, $\ddot{U}_{xo}$ and $\ddot{\phi}_{yo}$ can be approximated by $\ddot{U}^*_{xo}$ and $\ddot{\phi}^*_{yo}$, i.e. by the response of the foundation in absence of the superstructure. In this case Eq. (28) can be written in the form

$$\kappa_1(\omega) = \beta_1 \ddot{U}_{xg}(\omega) \left\{ \left[\frac{\ddot{U}^*_{xo}(\omega)}{\ddot{U}_{xg}(\omega)} \right] + 0.7 \left(\frac{H}{a} \right) \left[\frac{a\ddot{\phi}^*_{yo}(\omega)}{\ddot{U}_{zg}(\omega)} \right] \left[\frac{\ddot{U}_{zg}(\omega)}{\ddot{U}_{xg}(\omega)} \right] \right\} \tag{29}$$

Neglecting the small reduction of the horizontal motion of the foundation and using the standard value of 0.67 for the ratio of vertical to horizontal component of motion in the free-field leads to

$$\kappa_1(\omega) = \beta_1 \ddot{U}_{xg}(\omega) \left\{ 1 + 0.47 \left(\frac{H}{a}\right)\left(\frac{a}{20}\right) \left[\frac{a\ddot{\phi}_{yo}(\omega)}{\ddot{U}_{zg}(\omega)}\right]_{a = 20\ m} \right\} \qquad (30)$$

where a must be in meters.

By use of Eq. (30) and Figs. 9a, b and c, in which $|a\ddot{\phi}^*_{yo}(\omega)/\ddot{U}_{zg}(\omega)|$ is shown versus frequency, it is possible to estimate the effects of rocking. For example, for a typical containment structure in a nuclear power plant ($a = 20$ m, $H/a = 3$ and fixed-base natural frequency $f_1 = \omega_1/2\pi = 5$ Hz), the quantity within brackets in Eq. (30) takes the value 1.20 for a source at $r = 10$ km and $z_s = 5.5$ km. In this case, rocking of the foundation leads to a 20 percent increase in response of the superstructure. In the unlikely situation of a shallow source ($z_s = 1.0$ km) and short epicentral distance ($r = 1 - 10$ km), the effects of rocking would lead to a 30 percent increase in the response of the superstructure.

The ratio $|a\ddot{\phi}^*_{zo}/\ddot{U}_{zg}|$ for a source at $r = 10$ km and $z_s = 5.5$ km can be approximated by $0.14\,(f/5)(a/20)$. For multistory buildings, the fixed-base natural frequency f (in Hz) ranges from $40/H$ to $80/H$ where H is the total height in meters. With these approximations, the term within brackets in Eq. (30) can be found to lie in the range from 1.03 to 1.05. In this case, the effects of rocking would increase the response by less than 5 percent.

CONCLUSIONS AND DISCUSSION

It has been shown that it is possible to represent the free-field motion over a small region of the ground surface by the motion at a reference point within the region and by two "equivalent" frequency-dependent phase velocities. Sufficient information is available to estimate the frequency content of the motion at a point for a given magnitude, epicentral distance and type of soil condition. The "equivalent" phase velocities can be calculated from knowledge of the geologic structure, epicentral distance and source depth. The resulting model of the free-field motion, while preserving the most important characteristics of the ground motion, is simple enough to be determined by the information and analytic tools available. The model circumvents a more refined decomposition of the free-field motion in terms of different types of waves but is sufficiently general to account for the main effects of wave passage on surface foundations.

The estimates obtained for the effects of wave passage on extended rigid foundations indicate that the filtering effects on the translational components of motion are negligible for frequencies lower than 5 Hz. The filtering effects increase with frequency but become significant only at short epicentral distances from extremely shallow sources. The torsional response induced by the effects of wave passage while small is more pronounced. At a frequency of 5 Hz, the tangential motion on the perimeter of a square foundation of half-width $a = 20$ m can be of the order of 10 percent of the amplitude of motion in the free-field. It has been found that the

Uniform Building Code requirement of a minimum "accidental" eccentricity of 5 percent of the larger plan dimension is, in general, adequate to cover for the torsional effects of wave passage on symmetric structures. Exceptions are the cases of stiff structures (translational frequencies higher than 5 Hz) supported on foundations with lengths larger than 50 m. At short epicentral distances from extremely shallow sources it is also possible to find equivalent eccentricities higher than the minimum recommended by Code.

The effects of wave passage induce a small but significant rocking response component. At a frequency of 5 Hz, the vertical motion, induced by rocking, on the perimeter of a foundation of half-width $a = 20$ m can be of the order of 15 percent of the amplitude of the vertical component on the free-field. For flexible multistory buildings the increase in translational response of the superstructure caused by rocking of the foundation amounts to less than 5 percent. For stiffer structures, such as the containment building in nuclear power plants, the increase in response of the superstructure associated with rocking ranges from 20 to 30 percent depending on epicentral distance and source depth.

The effects of wave passage described above are based on estimates of these effects in the neighborhood on the fundamental frequencies of the structures considered. The higher modes are affected to a higher degree. The response of equipment mounted on structures may be sensitive to the higher frequency components of motion and requires a more complete analysis.

The estimates of the effects of wave passage obtained in this study should be considered as lower bounds of the magnitude of these effects. Several of the simplifications introduced tend to reduce the importance of the effects. In particular, the effects of the embedment of the foundation have been ignored. For embedded foundations the filtering of the translational response is more pronounced while the rocking response is augmented. The use of a horizontally layered model for the propagation medium tends to increase the estimates of the "equivalent" phase velocities resulting in a reduction of effects of wave passage. Heterogeneities in the real propagation path act as shallow secondary sources leading to lower "equivalent" phase velocities and more pronounced wave passage effects. The effects of embedment of the foundation can be analyzed by extending the representation of the free-field motion to account for variations width depth.

ACKNOWLEDGMENT

The work described here has been supported by Grant PFR 79.00006 from the National Science Foundation.

REFERENCES

Apsel, R. J., "Dynamic Green's Functions for Layered Media and Applications to Boundary-Value Problems," Ph. D. dissertation, Department of Applied Mechanics and Engineering Sciences, University of California, San Diego, 1979.

Eaton, J. P., M. E. O'Neill and J. N. Murdock (1970). Aftershocks of the 1966 Parkfield sequence, Bull. Seism. Soc. Am., 57, 1245-1257.

Heaton, T. H. and D. V. Helmberger (1978). Predictability of strong ground motion in the Imperial Valley: Modelling the M4.9, Nov. 4, 1976 Brawley earthquake, Bull. Seism. Soc. Am., 68, 31-48.

Iguchi, M. (1973). Seismic response with consideration of both phase difference of ground motion and soil-structure interaction, Proc. Japan Earthquake Engineering Symposium, Tokyo.

Kobori, T. and Y. Shinozahi (1975). Torsional vibration of structure due to obliquely incident SH wave, Prov. V. European Conference on Earthquake Engineering, No. 22, Istanbul, Turkey.

Lee, T. H. and D. A. Wesley (1975). Three-dimensional soil-structure interaction of nuclear structures during earthquakes considering ground rotational input, Proc. 2nd ASCE Specialty Conf. on Struct. Design of Nuclear Plant Facilities, New Orleans, Louisiana.

Luco, J. E. (1976a). Torsional response of structures to obliquely incident SH waves, Earthquake Engineering and Structural Dynamics, 4, 207-219.

Luco, J. E. (1976b). Torsional response of structures for SH waves: the case of hemispherical foundations, Bull. Seism. Soc. Am., 66, 109-123.

Luco, J. E. and H. L. Wong (1979). Response of structures to non-vertically incident seismic waves, Report Dept. of Appl. Mechs. and Engineering Sciences, University of California, San Diego.

Luco, J. E. and R. J. Apsel (1980). On the Green's functions for layered media: Part I (submitted for publication).

McGuire, R. K. (1978). A simple model for estimating Fourier Amplitude Spectra of horizontal ground acceleration, Bull. Seism. Soc. Am., 68, 803-822.

Newmark, N. M. (1969). Torsion of symmetrical buildings, Proc. 4th World Conference on Earthquake Engineering, Santiago, Chile.

Scanlan, R. H. (1976). Seismic waves effects on soil-structure interaction, Earthquake Engineering and Structural Dynamics, 4, 379-388.

Tani, S., J. Sakurai and M. Iguchi (1973). The effect of plane shape and size of buildings on the input earthquake motion, Proc. 5th World Conference on Earthquake Engineering, Rome.

Trifunac, M. D. (1976). Preliminary empirical model for scaling Fourier Amplitude Spectra of strong ground acceleration in terms of earthquake magnitude, source-to-site distance, and recording site conditions, Bull. Seism. Soc. Am., 66, 1343-1373.

Wong, H. L. and J. E. Luco (1976). Dynamic response of rectangular foundations to obliquely incident seismic waves, Earthquake Engineering and Structural Dynamics, 4, 379-388.

Wong, H. L. and J. E. Luco (1978). Tables of impedance functions and input motions for rectangular foundations, Report CE78-15, Dept. of Civil Engineering, University of Southern California, Los Angeles, California.